

# The Structural Features of Soil Temperature and Precipitation and Soil Heat Flux Fields of Strong Earthquakes

Fan Xin-gang and Tang Mao-cang

Lanzhou Institute of Plateau Atmospheric Physics, Academia Sinica, Lanzhou 730000, China

A typical distribution pattern of soil temperature and precipitation field has been discovered in areas of strong earthquakes ( $M_s \geq 7.0$ ). A positive soil temperature anomaly existed in the epicentral area of the forthcoming earthquake for 1/2 to 1 year before the earthquake; meanwhile, a relatively large negative soil temperature anomaly appeared in the surrounding area. Similarly, there was a small pluvial region in the epicentral area during the period of 1-5 months before the earthquake, while the background was dry. The area of positive soil temperature anomaly and the pluvial region expanded and strengthened gradually with time.

Based on these facts, a new method to calculate soil heat flux by using soil temperature data of meteorological stations was designed, which can filter out the influence of atmosphere and obtain the information on the geothermal field in deep earth. In this paper, the soil heat flux of about 200 stations in the areas of six strong earthquakes (four in the People's Republic of China and two in Mongolian People's Republic) has been calculated, from which it can be seen that a typical geothermal structure exists under the earth surface. The heat flux in the epicentral area of a forthcoming earthquake is upward, while in the surrounding area it is downward. The geothermal structure has some influence on soil temperature and the precipitation field.

**Key words:** Earthquake, Soil temperature field, Precipitation field, Soil heat flux, Three-dimensional thermal column structure.

## I. INTRODUCTION

At present, the subjects in the earth sciences, such as seismology, geophysics and modern climatology, are developing toward becoming interdisciplinary. There have been some studies about the relationships between geothermal fields and earthquake fields, earthquakes and geothermal anomalies [1], soil heat and climate [2], and earthquakes and precipitation [3]. Earthquakes, soil temperature, precipitation, and deep layer geothermals are interrelated and interactive. Thus any of the above problems need other factors to be considered simultaneously, i.e., they must be put into the same system (geo-system) to be studied comprehensively and to probe the relationship among the factors.

**Table 1**  
Six earthquakes occurred in North China and Mongolia.

Order	Date	Epicentral location	Longitude (E)	Latitude (N)	Magnitude
1	1966-03-22	Xingtai	115.1°	37.5°	7.2
2	1969-07-18	Bohai Sea	119.4°	39.2°	7.4
3	1976-07-28	Tangshan	118.7°	39.4°	7.8
4	1989-10-18	Datong	113.9°	40.0°	6.1
5	1957-12-04	Mongolia No.1	99.2°	45.2°	8.0
6	1967-01-05	Mongolia No.2	102.9°	48.2°	7.5

Note: The order is the same in this paper.

In this paper, by utilizing the soil temperature and precipitation data from meteorological stations in China and the Mongolia People's Republic compiled by the fourth division of the Lanzhou Institute of Plateau Atmospheric Physics of the Chinese Academy of Sciences, the structural features of soil temperature fields, precipitation fields, and shallow soil heat flux fields in the areas of six strong earthquakes (see Table 1) that occurred in North China and Mongolia are comprehensively analyzed.

## II. FEATURES OF SOIL TEMPERATURE FIELDS

By analyzing monthly soil temperature anomaly figures at a depth of 1.6 m and 3.2 m, it is found that a distribution pattern, that is, a positive anomaly in the epicentral area surrounded by a negative anomaly belt, maintained for a long period from several to more than 10 months before the earthquake. In ordinary circumstances, the positive anomaly area is a smaller area that occurred in the large negative anomaly area. Figure 1 shows the distribution of 3.2 m soil temperature anomalies of the third month after this kind of pattern occurred before each strong earthquake. It is also found that this kind of distribution pattern of the soil temperature field has appeared 9, 8, 7, 6, 12, and 11 months, respectively, before the strong earthquakes, and there are very obvious matched positive-negative distribution patterns of soil temperature anomaly around every earthquake epicenter. Among these, for example, the soil temperature pattern before the Xingtai earthquake is the most obvious and characteristic one, in which the positive anomaly area in the center is almost entirely surrounded by the negative one. Before the Mongolia No. 1 *M*, 8.0 earthquake, although soil temperature stations are sparse, the matched positive-negative distribution pattern still existed from referring to the distribution of soil temperature field in the surrounding regions of China, and it occurs early, its range is large, and its negative area expands to most parts of China.

From further analysis of the features of the above soil temperature fields, it is found that the area and central intensity of the positive anomaly area obviously changes with time. For the sake of easy

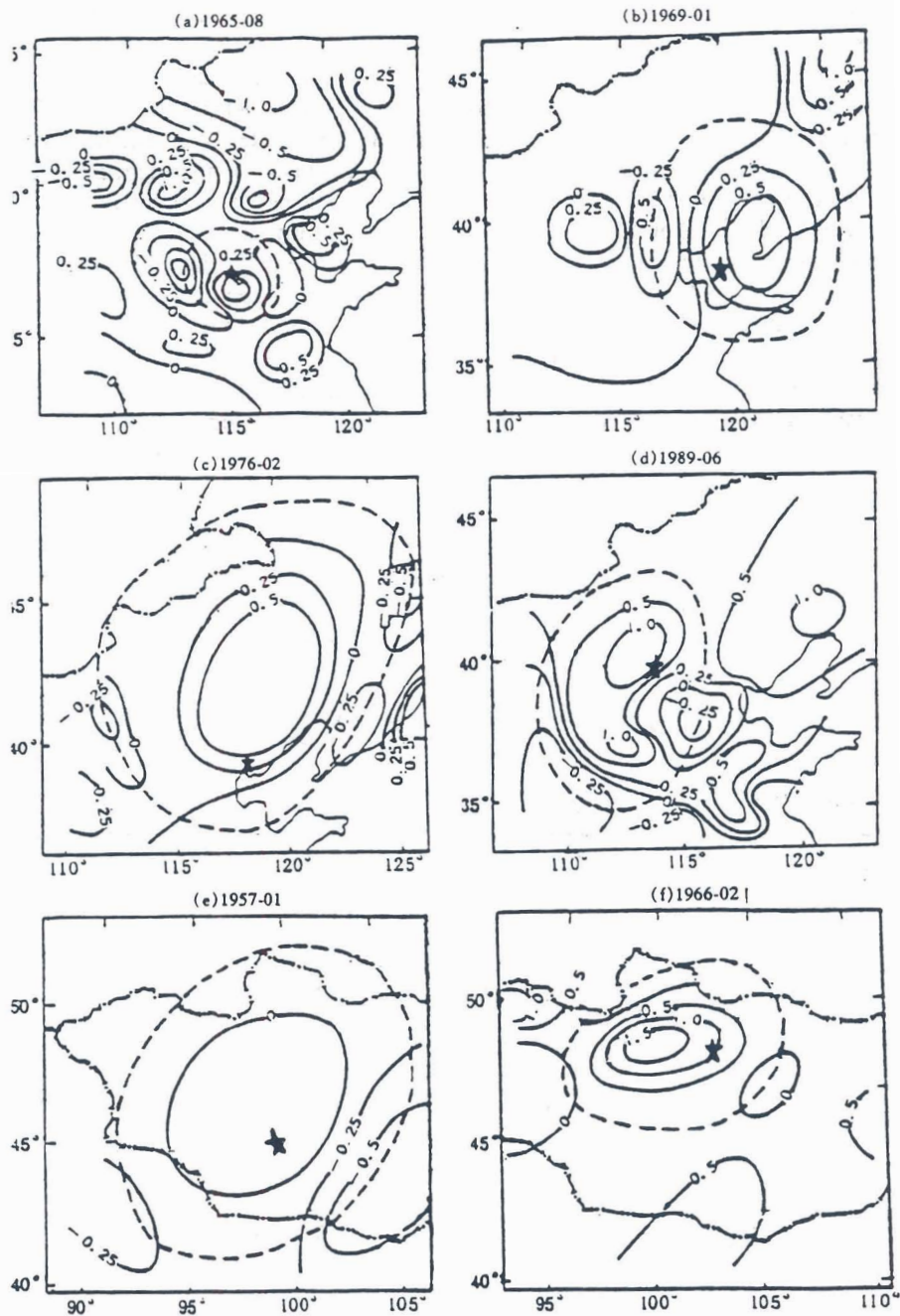


**Fig. 1**

The isoline figure of the 3.2 m monthly soil temperature anomaly (Unit: °C). The dashed lines are the axis lines of the negative anomaly belt. ★ represents for the coming epicenter.

illustration, take the mean of the long and short axis of the area surrounded by a negative anomaly belt (see Fig. 1) to represent its area, and take the central soil temperature anomaly value in the positive anomaly area to express central intensity. Then their evolution curves at 3.2 m are shown in Fig. 2 (Bohai Sea earthquake and Mongolian No.1 earthquake are not shown due to rare data). From this we can find their common rule, that is, a considerable positive soil temperature anomaly occurs in several months before the earthquake occurrence, and with the earthquake approaching, the positive anomaly area enlarges gradually and its intensity also enhances continuously. When the earthquake occurs, the area reaches the maximum and the intensity is still maintained. After the earthquake, the area and intensity of the positive anomaly return to normal in several months, and the matched positive-negative pattern also disappears. The area (diameter) surrounded by the negative anomaly area is about 300 km to 1500 km; in general, it is about 1000 km. The maximum of central intensity can reach about 0.2°C. The above facts demonstrate that the time scale of the earthquake is relatively short (from several months to several years) and its space scale is also fairly small (about 1000 km). Moreover, the earthquake magnitude and the area and central intensity of the high temperature area approximately assume a positive correlative relationship.

In a word, all the shallow layer soil temperature fields around strong earthquakes of  $M_s \geq 7$  (Datong earthquake is  $M_s$ , 6.1) in North China and its neighboring north area during the 40 years

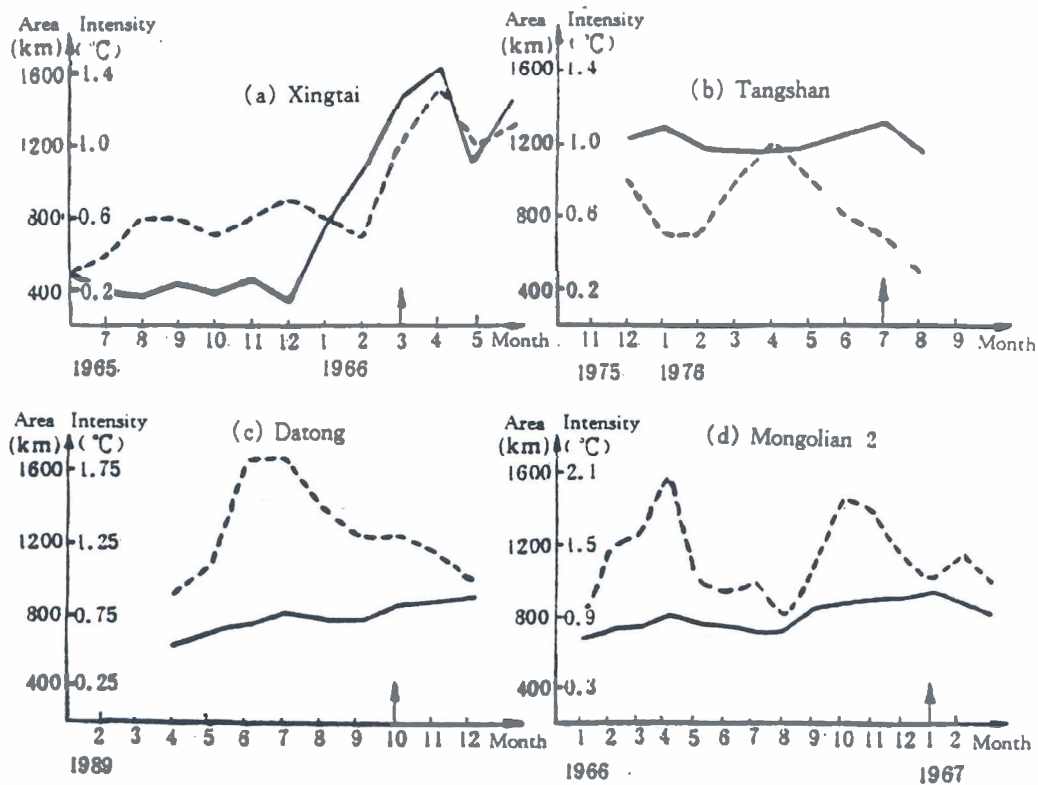


Fig. 2

The evolution curve of the area and central intensity of the region surrounded by negative anomaly belt on 3.2 m soil temperature field. The solid line represents for area (Unit: km), the dashed line expresses central intensity (Unit: °C), and † represents earthquakes.



studied by us have the above features, which are called a "seismogenic soil temperature field."

Not only are strong earthquakes accompanied by "seismogenic soil temperature fields", but also some small earthquakes. For example, of the soil temperature anomaly figures from May to November of 1989, all 27 earthquakes of  $M \geq 5$  on the Chinese continent and its margin area from April in 1989 to March in 1990 occurred in the positive soil temperature anomaly area. Figure 3 shows the 3.2 m soil temperature anomaly field of September in 1989 and the earthquake distribution. This indicates that the "seismogenic soil temperature fields" of Chongqing earthquake and Datong earthquake are very obvious.

### III. FEATURES OF PRECIPITATION FIELDS

Generally, the above "seismogenic soil temperature field" maintains for several months to several years. It forms a special sub-boundary condition in the atmosphere as well as a considerable external force source. According to Maocang Tang's study [2], there is a fairly good correspondence relation between the soil temperature field in a time period and the precipitation field in the following period. So it is conceived that the "seismogenic soil temperature field" would have an effect on the precipitation field. The monthly and annual precipitation in relation to earthquakes is also analyzed. Figure 4 shows the annual precipitation anomaly percentage distributions for the year before five earthquakes (an earthquake occurred after October is classified in next year [4]). It can be found that a large-scope drought occurs during the year before earthquakes; however, a small-area weak positive anomaly (or weak negative anomaly) exists at the same time in the epicentral area. Especially for the Mongolian No. 1 earthquake on December 4, 1957 (Fig. 4e), the drought area extended to Inner Mongolia, Gansu, Shanxi, Hebei, and other provinces of China; meanwhile a quite small pluvial area existed in the epicenter. It can be seen from Fig. 4d that there is a large drought area around Datong including Shanxi, Inner Mongolia, Hebei, Henan, Shanxi, and Shandong provinces; interestingly, a pluvial area in Qinghai and Gansu provinces extends eastward via Inner Mongolia to Datong, making it a small pluvial area in the large-scope partial rain area. In 1965, the year before the Xingtai earthquake, most parts of North China were dominated by drought (Fig. 4a). Although it was dry around Xingtai, the annual precipitation anomaly percentage was greater than -50% and formed a small weak drought area; in other words, the precipitation was relatively more than that in the area around it. Analogous cases of precipitation field occurred in the year before the Bohai Sea and Tangshan earthquake (Fig. 4b,c). Since the features of the soil temperature field before the Mongolian No. 2 earthquake appeared very early, this kind of anomalous precipitation field had appeared 2 years before the earthquake. Figure 4f gives the annual precipitation anomaly percentage distribution in 1965, from which it can be found that there is an obvious small pluvial area in the coming epicenter and a large-scope drought area around it.

Through analyses of the monthly precipitation anomaly percentage figures in the months before each earthquake, it can be seen that, in a common situation, the precipitations are all small and the rainy situations appear only during a few months in the forthcoming epicenter; the pluvial area appears from 1 to 5 months before earthquake occurrence in the forthcoming epicenter, and with the earthquake approaching, the rain intensity enhances; after the earthquake, the rain area spreads and enlarges quickly and forms a large-scope rainy area. Figure 5 shows the monthly precipitation anomaly percentage distributions of 3 months before the Xingtai earthquake and 1 month after it. It is shown that a weak rainy center appeared in the forthcoming epicenter in January 1966, then the rain area expanded and intensity enhanced somewhat in February, and until March of the year, the rain area expanded quickly and the intensity obviously enhanced. We call this kind of precipitation field a "typical pre-earthquake precipitation field." It cooperates with the "seismogenic soil temperature field" and tallies with the "drought-earthquake relation" raised by Qingguo Geng [3] in large area and long time scale; moreover it is also a correction and supplement for the "drought-earthquake relation." This will be beneficial to improve the precision of short-term earthquake prediction.

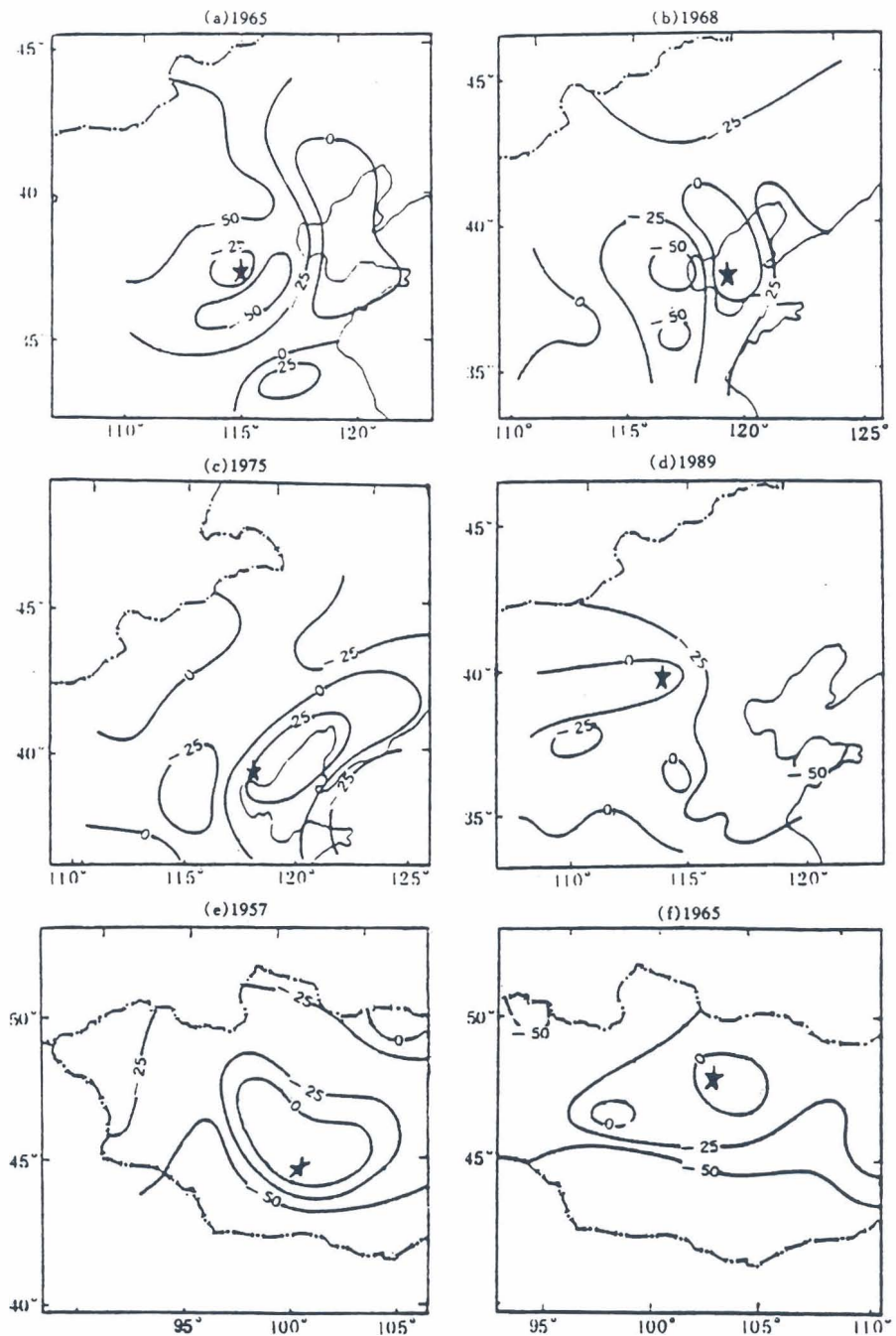


**Fig. 4**  
Distributions of annual precipitation anomaly percentage (%). ★ represents for the coming epicenter.

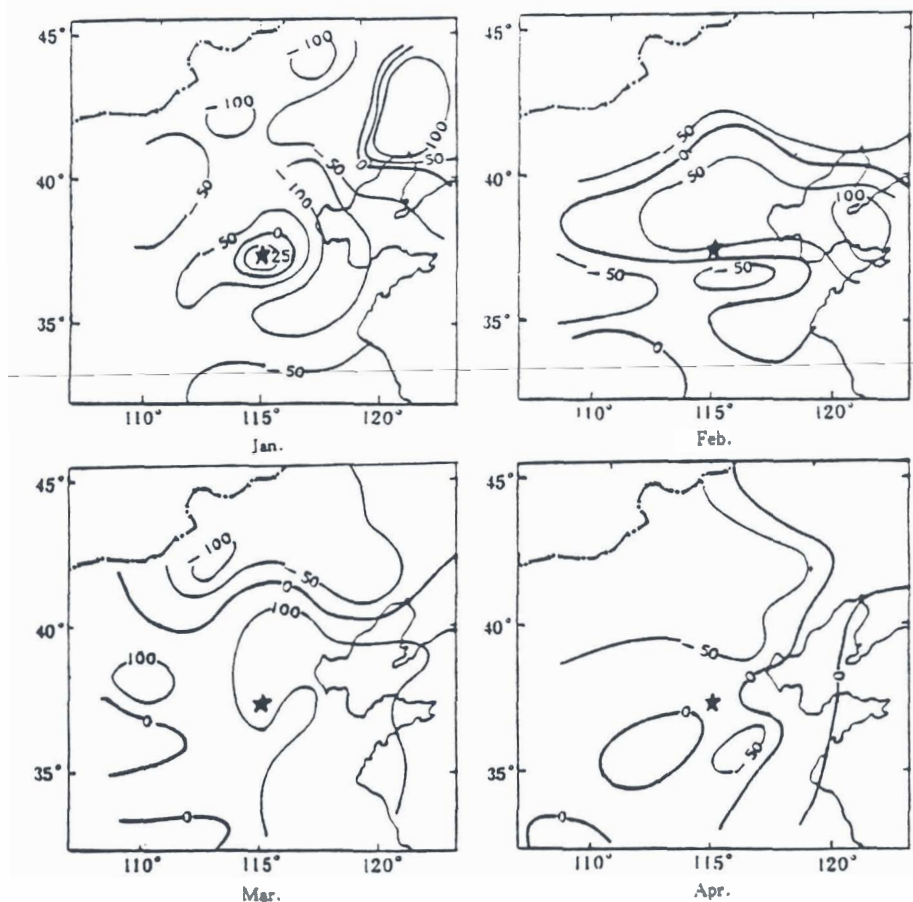


Fig. 5

Distributions of monthly precipitation anomaly percentage from January to April in 1966 (%). ★ represents for the coming epicenter.

#### IV. EARTHQUAKE AND SHALLOW LAYER SOIL HEAT FLUX

It is well known that the energy of outward thermal flow from the deep layer of the internal earth is a fundamental variate in the earth energy balance. There are three ways to transmit the geothermal flow: conduction, convection, and radiation. Among them the most common way is conductive transmission. At present, geothermal flow data in geology are obtained from drilling temperature surveys as well as rock thermal conductivity. Because of the expensive costs and small quantity, this method can not satisfy the needs of large-scale studies. Fortunately, it is possible for people to use the soil temperature data of meteorological stations for the purpose of conjecturing the geothermal flux from the deep layer after suitable mathematical processing. Though the depth is somewhat shallow (the maximum depth is 3.2 m), the stations are dense (there are 200 stations all over China) and the observation time is longer than several decades. In this paper, the soil temperature data of three layers from meteorological stations of 0.8 m, 1.6 m, and 3.2 m are used to calculate the shallow layer soil heat flux, and then the features of the distributions and changes of shallow layer soil heat flux during the seismogenic period of strong earthquakes are analyzed.

The problem of vertical one-dimensional geothermal transmission, without taking into account the heat source (sink), was simply considered here. According to reference [5], the quantity of one-dimensional conductive thermal flow is

$$Q_d = -\rho c \kappa \frac{\partial T}{\partial z} \quad (1)$$

where  $\rho$  is medium density and  $c$  is specific heat (in general they can be assumed as constant); the volume thermal capacity was given as  $C_w = \rho c = 1.256 \text{ J}\cdot\text{cm}^{-3}\cdot\text{K}^{-1}$  by Tang et al. [6].  $\kappa$  is the medium thermal diffusivity,  $T$  is soil temperature,  $z$  is the vertical coordinate, and  $\frac{\partial T}{\partial z}$  is the soil temperature gradient (it is replaced by difference in calculation,  $\frac{\partial T}{\partial z} \approx \frac{\Delta T}{\Delta z}$ ). The negative sign indicates that the direction of thermal flow is opposite to that of the soil temperature gradient.

### 1. The Calculation of Soil Heat Flux

The one-dimensional linear thermal conductive equation was given by G. Buntebarth (1984) as

$$\frac{\partial T}{\partial t} = \kappa \frac{\partial^2 T}{\partial z^2} \quad (2)$$

Generally, this is a problem in half-space without an initial condition in geothermal studies. When given an amplitude  $A$ , a circular frequency  $\omega$ , and an initial phase  $\beta$ , a wave boundary condition then can be given as follows:

$$T(z_0, t) = \bar{T} |_{z=z_0} + A \sin(\omega t + \beta)$$

where  $\bar{T}$  is mean temperature at  $z = z_0$ . Its disturbed quantity  $T = T - \bar{T} = A \sin(\omega t + \beta)$  also satisfies Eq. (2); the analytical solution of equation (2) can be written as

$$\begin{aligned} T(z, t) &= T(z, t) - \bar{T} |_{z=z_0} \\ &= A \exp \left[ -(z - z_0) \sqrt{\frac{\omega}{2\kappa}} \right] \cdot \sin \left[ \omega t - (z - z_0) \sqrt{\frac{\omega}{2\kappa}} + \beta \right] \end{aligned} \quad (4)$$

It is shown that the amplitude and the phase of boundary wave change with depth and are related to thermal diffusivity  $\kappa$  and circular frequency  $\omega$ . Conversely, according to the changes of amplitude ( $A$ ) and phase ( $\Phi$ ) at a given frequency, the thermal diffusivity  $\kappa$  can be determined

$$\kappa = \frac{\omega}{2} \left[ \frac{(z_2 - z_1)}{\ln(A_2/A_1)} \right]^2 \quad \text{or} \quad \kappa = \frac{\omega}{2} \left[ \frac{z_2 - z_1}{\Phi_2 - \Phi_1} \right]^2 \quad (5)$$

#### (1) The calculation of the thermal diffusivity $\kappa$ ( $\text{cm}^2/\text{s}$ )

The calculation of the geothermal flow in a geological department utilizes the observational deep layer rock thermal conductivity; this is not suitable for large-scale and varying soils in our meteorological department, especially for the calculation of shallow layer soil heat flux in this study. So Eq. (5) is used to compute the thermal diffusivity.

After analyzing the 0.8-3.2 m soil temperature data, it was found that the variance contribution of the annual wave among three layers is the largest, that of most stations exceeded 98%, and the smallest one also exceeded 95%. This fact satisfies fundamentally the wave boundary condition required in Eq. (5). So the value of  $\kappa$  can be calculated by utilizing the ratio of amplitudes or the difference in phases of the annual wave in soil temperature data series at 0.8 and 3.2 m (the range of 0.8-3.2 m includes the two layers of 0.8-1.6 m and 1.6-3.2 m). From Eq. (5) we find that only one  $\kappa$  can be obtained at a period  $t_0$  ( $t_0 = 2\pi/\omega$ ). However, in fact, the thermal diffusivity is different in winter and in summer as affected by temperature and humidity. In accordance with this,  $\kappa$  is calculated separately in this paper so that the calculated value is more realistic. One-year data is divided into summer and winter sections to fit the annual wave, respectively, to obtain the amplitude and phase. Certainly, we should take each section as close to the peak as possible to improve fitting precision when dividing sections. According to the distribution of phase of observational soil temperature series, the two sections are taken as the summer section from May to October and the winter section from November to next April at 0.8 m; at 3.2 m, the summer section is from July to December and the winter section is from January to June. As we know, the transmission of the annual wave from 0.8 m to 3.2 m needs about 2 months; this kind of data division is therefore close to the reality. After dividing the sections, half-year data is fit with the annual wave by utilizing the least square method to get amplitude and phase; then the thermal diffusivities in summer and winter can be gained from Eq. (5). Because there exists a permafrost layer in some areas, such as Northeast China and Tibet, and there exists influences of soil humidity in some other areas, the calculated  $\kappa$  is unstable in some stations. To deal with this phenomenon, the area smoothing method is used; thus,  $\kappa$  of these stations can be gained from the stations around them by interpolation. In this paper,  $\kappa$  takes the mean value of the decade during which each earthquake occurs to calculate conductive heat flux.

## (2) The Calculation of Shallow Layer Soil Heat Flux

When the positive direction is given as upward, according to Eq. (1), the quantity of transmission flux is

$$Q_d = \rho c \kappa \frac{\partial T}{\partial z} \approx C_w \kappa \frac{\Delta T}{\Delta z} \quad (6)$$

Here  $\frac{\Delta T}{\Delta z}$  can be simply gained from two layers of soil temperature, and the calculation of heat flux is easy. But this heat flux contains both influences coming from the earth surface and the deep layer. According to Maocang Tang et al. [6], the distribution pattern of normals of soil heat flow is very similar to that of the deep-layer geothermal flow field in the earth. Additionally, as above, the earthquake occurred with deep earth influences on soil temperature field and precipitation field. This suggests that the thermal flow from the deep layer is a variate that could not be neglected, both for accumulation effect on the long time-scale and direct effect to climate on the short time-scale.

It can be seen from the analytic solution (4) of the thermal conductive equation that the wave amplitude decreases exponentially with depth. According to G. Buntebarth [5], the depth where the maximum change of temperature (amplitude) decreases to 1/e of that at surface is defined as the maximum transmission depth of the periodic wave at the earth surface and is denoted as  $z^*$ ; then

$$z^* = \sqrt{\frac{2\kappa}{\omega}} \quad (7)$$

When an intermediate value for  $\kappa$  is given as  $\kappa = 5.5 \times 10^{-3} \text{ cm}^2/\text{s}$ , the maximum transmission depth of daily change and annual change of surface temperature are, respectively, 0.12 m and 2.35 m. In fact, at a depth of 0.28 m and 5.4 m, the influence of daily change and annual change is still 1/10 of

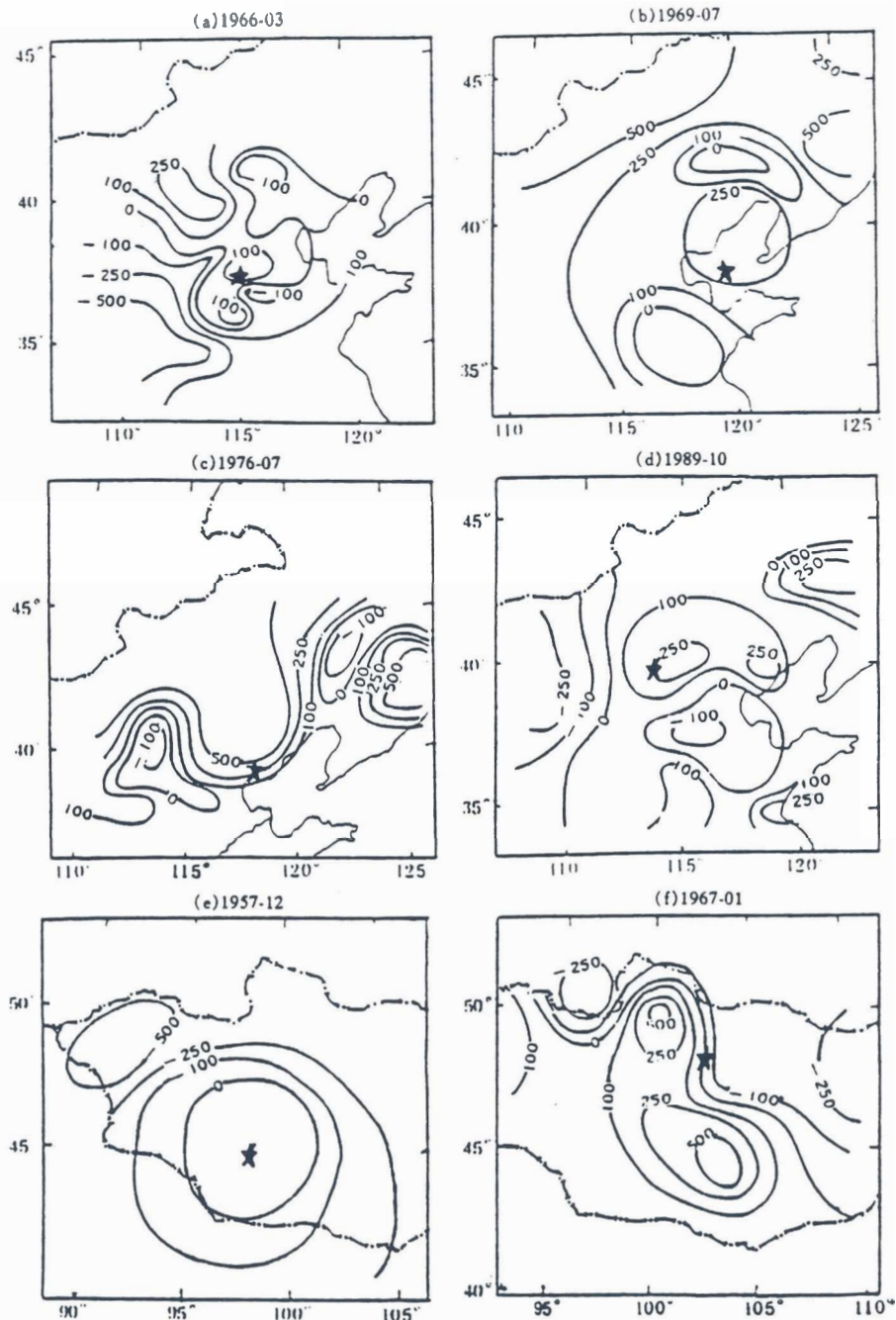


**Fig. 6**  
The distributions of monthly soil heat flux when each earthquake erupts ( $\text{mW}/\text{m}^2$ ). ★ represents for the epicenter.

that at the surface. So it can be concluded that the influence of the surface annual wave on the deep layer is considerably large. Even for the half-year wave, its influence at a depth of 3.8 m is 1/10 of that at surface, and the wave period is longer and its influence depth is deeper. In order to gain the information of the soil thermal field in deep earth, the influence of the surface wave must be filtered out.

It is known from Eq. (6) that in order to compute the soil heat flux that can reflect the information of the deep layer thermal field, the soil temperature gradient  $\frac{\Delta T}{\Delta z}$  induced by the influence of thermal transmission from deep layer must first be obtained. From the study of Hu Ze-yong et al. [7], the soil temperature wave propagates in two ways. Generally, a short wave propagates downwards and the phase of the upper layer is ahead of the lower layer, and a long wave (2 years or more) propagates upwards and the phase of the lower layer is ahead of the upper layer. So during the period of earthquakes studied in this paper, the soil temperature data of meteorological stations of 2 years before earthquake and 1 year after earthquake was selected to perform the computation. The computational steps are as follows:

i) By utilizing the periodogram analysis method, analyze the 0.8 m soil temperature series to gain the amplitude and phase of key waves that exist with a reliability of 99%; their periods are in the range of 2 to 18 months.

ii) According to formula (4), compute the soil temperature ( $T'_{1.6}$  and  $T'_{3.2}$ ) of these waves propagated to 1.6 m and 3.2 m. They are the influences of a 0.8 m wave on the two layers.

iii) From the real soil temperature series of 1.6 m and 3.2 m, subtract the influences of the 0.8 m wave; then gain the soil temperature series  $T^*_{1.6}$  and  $T^*_{3.2}$  of 1.6 m and 3.2 m induced by the thermal transmission under 3.2 m alone.

$$T^*_{1.6} = T_{1.6} - T'_{1.6} \quad T^*_{3.2} = T_{3.2} - T'_{3.2} \quad (8)$$

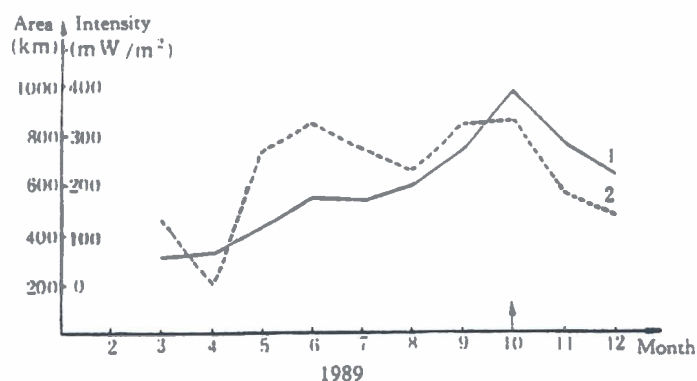
iv) Compute the soil temperature gradient from 1.6 m to 3.2 m:

$$\frac{\Delta T}{\Delta z} = \frac{(T^*_{3.2} - T^*_{1.6})}{160} \quad (^\circ\text{C}/\text{cm})$$

v) Using formula (6), it is easy to compute the soil heat flux that reflects the information of the geothermal field of deep earth. The upward heat flux is assigned a positive.

## 2. Analysis of Results

We have calculated the monthly shallow soil heat flux field around each earthquake, respectively; its distribution has a general rule during earthquake. The epicentral area is the region of positive heat flux in which heat flow is upwards, and there is a belt of negative heat flux surrounding the epicentral area, in which heat flow is downward; thus a kind of heat flux column is composed in a three dimensional structure. Most earthquakes occur near the edge of positive heat flux region, namely, the region of high horizontal gradient of heat flux. Figure 6 shows the distribution of soil heat flux when each earthquake occurs; we can see the above pattern of distribution. In order to research the rules of time evolution, we take the mean of the long and short axis of the region surrounded by the axis line of negative heat flux belt as the range of positive heat flux and take the highest heat flux quantity in positive heat flux region as its central intensity. Figure 7 shows the evolution curve of the central intensity and the range of positive flux region of the Datong earthquake, which has the most abundant data. From Fig. 7 it is found that this kind of distribution, in which positive and the negative heat flux region match each other, appears from 9 months before the earthquake and maintains until 2 months after. The range of positive heat flux region in the epicentral area gets larger and larger while closing



1989  
Fig. 7

The evolution curve of the range and the central intensity of the region surrounded by negative soil heat flux belt during Datong earthquake. Solid line represents range (Unit: km), dashed line expresses central intensity ( $\text{mW}/\text{m}^2$ ), and  $\uparrow$  represents the earthquake.

to the earthquake, and the central intensity shows a generally increasing trend. Just after the earthquake, the area of the positive region grows larger again. This kind of distribution disappears in the later short time. We can name the soil heat flux field having this kind of construction and evolutionary features as "seismogenic soil heat flux field."

## V. DISCUSSION

From the above calculations and results, we can conclude that soil temperature field, precipitation field, and shallow soil heat flux field all have obvious evolutionary features of structure during a seismogenic period. The soil heat flux field, of which the heat flow is upward in the epicentral area and downward in the peripheral area, forms a three-dimensional soil heat column structure called the "seismogenic soil heat flux field." Its spatial range and intensity increases gradually with the earthquake's coming. Meanwhile, after accumulating for some time, the shallow soil temperature field changes. The forthcoming epicentral area becomes a positive soil temperature anomaly area since the soil temperature is increasing with accumulating geothermal energy and the peripheral belt becomes a negative soil temperature anomaly belt since the temperature is decreasing as energy is lost. These two form the "seismogenic soil temperature field." Thus the atmosphere over this kind of boundary layer shows some responses after some time, the partial rain area accords with the large area of negative soil temperature anomaly, and the pluvial area accords with the positive soil temperature anomaly region. Now the distribution of the precipitation field has a weak rainy center in the forthcoming epicentral area under the background of a large range drought before earthquake. Moreover, precipitation increases 1 to 5 months before earthquake and 1 to 3 months after the earthquake; then the "typical pre-earthquake precipitation field" is formed. On eruption of the earthquake, all the earthquake energies release in a comparatively short time. As a result, the shallow soil heat flux field shows a comparatively large range positive heat flux region. As we know, the shallow soil heat flux field mainly contains the information of the deep layer geothermal field, so that a series of courses of energy transmission, release, and transformation etc. are related to the changes of the deep layer geothermal field before an earthquake. According to the study of Rongsheng Zeng et al. [8], the transverse irregularity of top mantle temperature leads to a break in Moho discontinuity; some breaks have previously existed. Warm materials in the mantle can rise into the crust through

these breaks. Therefore, the focus of an earthquake becomes a heat source due to the intrusion of warm material; this phenomenon is consistent with the features shown by the "seismogenic soil temperature field" and the "seismogenic soil heat flux field."

This paper discussed how to obtain information on the deep layer geothermal field from the data of shallow soil temperature and analyzed the relationships between this information and the soil temperature field and the precipitation field during an earthquake. However, only conductive transmission of heat was considered here; as a matter of fact, convective transmission also plays a role during an earthquake. This will be discussed in another paper. Furthermore, only six strong earthquakes that have comparatively intensive data were discussed in this paper; other earthquakes and geophysical phenomenon related to deeper earth are waiting for further studies.

#### REFERENCES

- [1] Моисеенко, Y.N., (Russian), Ranalli, G. et al., (translated by Gao Li-qing, Chen Peng-nian, and Chen Hong-de,) Research and Application of Geothermal, Beijing, Seismological Press, 1990.
- [2] Tang Mao-cang et al., Theoretical Climatology, Beijing: Meteorological Press, 1989.
- [3] Geng Qing-guo, Research of Relationship Between Drought and Earthquake in China, Beijing, Marine Press, 1985.
- [4] Tang Mao-cang and Hu Zong-hai, Statistical analysis of strong earthquake influencing precipitation, *Northwestern Seismological Journal* (in Chinese), 12 (1), 19-29, 1990.
- [5] Buntebarth, G., Translated by Yi Zhi-xin, Xiong Liang-ping, Introduction of Geothermal, Beijing, Seismological Press, 1988.
- [6] Tang Mao-cang, Dong Wen-jie, Wang Bao-ling, et al., Comparison of soil heat flow field in China with deep layer geothermal field, *Advances of Earth Science*, 6(4), 10-17, 1991 (in Chinese).
- [7] Hu Ze-yong and Tang Mao-cang, Abnormality of Geothermal is an Important Factor of Climatic Abnormality, Comprehensive Research of Sky-earth-biology, Beijing, Chinese Scientific and Technological Press, 257-260, 1989.
- [8] Zeng Rong-sheng, Zhu Lu-pei, He Zheng-qing, et al., A seismic source model of the large earthquakes in north china extensional basin and discussions on the genetic processes of the extensional basin and earthquakes, *Acta Geophysica Sinica* (in Chinese), 34, 288-301, 1991.